Structure and interaction in the polymer-dependent reentrant phase behavior of a charged nanoparticle solution

Sugam Kumar,[1] D. Ray,[1] V. K. Aswal,[1] and J. Kohlbrecher[2]
[1]*Solid State Physics Division, Bhabha Atomic Research Centre, Mumbai 400 085, India*
[2]*Laboratory for Neutron Scattering, Paul Scherrer Institut, CH-5232 PSI Villigen, Switzerland*
(Received 29 July 2014; published 31 October 2014)

Small-angle neutron scattering (SANS) studies have been carried out to examine the evolution of interaction and structure in a nanoparticle (silica)–polymer (polyethylene glycol) system. The nanoparticle-polymer solution interestingly shows a reentrant phase behavior where the one-phase charged stabilized nanoparticles go through a two-phase system (nanoparticle aggregation) and back to one-phase as a function of polymer concentration. Such phase behavior arises because of the nonadsorption of polymer on nanoparticles and is governed by the interplay of polymer-induced attractive depletion with repulsive nanoparticle-nanoparticle electrostatic and polymer-polymer interactions in different polymer concentration regimes. At low polymer concentrations, the electrostatic repulsion dominates over the depletion attraction. However, the increase in polymer concentration enhances the depletion attraction to give rise to the nanoparticle aggregation in the two-phase system. Further, the polymer-polymer repulsion at high polymer concentrations is believed to be responsible for the reentrance to one-phase behavior. The SANS data in polymer contrast-matched conditions have been modeled by a two-Yukawa potential accounting for both repulsive and attractive parts of total interaction potential between nanoparticles. Both of these interactions (repulsive and attractive) are found to be long range. The magnitude and the range of the depletion interaction increase with the polymer concentration leading to nanoparticle clustering. At higher polymer concentrations, the increased polymer-polymer repulsion reduces the depletion interaction leading to reentrant phase behavior. The nanoparticle clusters in the two-phase system are characterized by the surface fractal with simple cubic packing of nanoparticles within the clusters. The effect of varying ionic strength and polymer size in tuning the interaction has also been examined.

DOI: 10.1103/PhysRevE.90.042316 PACS number(s): 82.70.Dd, 82.35.Np, 61.46.−w, 61.05.fg

I. INTRODUCTION

Nanoparticle-polymer systems have gained much attention in both the scientific and industrial communities, as they are known to show rich phase behavior having numerous applications in fields ranging from biotechnology (e.g., targeted drug delivery, biosensors, diagnostics, etc.) to the design of new hybrid functional materials [1–5]. Many of these applications require understanding of the various interactions present in the system and the corresponding phase behavior as a function of solution conditions, so that the desirable properties may be obtained [6,7]. In general, the presence of polymers in the solution of nanoparticles may either stabilize the nanoparticles through steric repulsion or destabilize by depletion attraction depending upon the system conditions [8–12]. Steric repulsion emerges as a result of polymer adsorption on the nanoparticle surface, whereas the nonadsorbing nature of polymers leads to depletion attraction. In fact, depletion interactions are unambiguously known to arise in the mixtures of two significantly different sizes of colloidal particles, when the smaller one experiences an excluded volume interaction with the larger one. The understanding of depletion interaction is typically based on a pseudo-one-component description where the reduction in polymer density between the particles gives rise to an osmotic pressure imbalance resulting in a net particle attraction of entropic origin. In those approaches, the effect of the free polymers on the particles is described in terms of a pair potential whose strength is governed by polymer concentration and range characterized by the polymer radius of gyration R_g [12–16]. As the polymer concentration increases towards the semidilute or overlap concentration, and/or R_g is not much less than particle radius (R), the polymer-polymer interactions become important. In these cases, treating the polymers with negligible interaction between them becomes an increasingly poor approximation. Ignoring these physical constraints results in an overestimation of the polymer-induced depletion attraction in the classical approaches [13,15].

The different models for depletion attractions predict monotonic growth in the strength of depletion attractions with increasing polymer concentrations [16–18]. However, a colloidal dispersion which is destabilized at low polymer concentrations due to depletion attraction may restabilize at high concentrations due to so-called depletion stabilization [19–21]. The evolution of depletion attraction is reasonably understood, but the formalism of the stabilization effect is still a subject of debate. One understanding is that stability arises due to the presence of repulsive maxima in the free energy curve of interaction between the particles at high polymer concentrations [21]. The presence of other forces such as electrostatic repulsion and/or polymer-polymer repulsion (nonideality of the polymer molecules) is also found to give rise to a positive potential barrier in combination with an attractive well in the depletion interaction [22–25]. On the other hand, there are some studies assuming that depletion interactions are purely attractive [16,17], and the depletion restabilization at higher concentrations is solely due to the decrease of the depletion layer thickness leading to weaker depletion attraction [26]. For understanding nanoparticle-polymer phase behavior, it is therefore of interest to look into the evolution of depletion interaction of nanoparticles in the presence of a wide range of polymer concentrations.

In this paper, we have observed a reentrant phase behavior in nanoparticle-polymer systems where one-phase charged stabilized silica nanoparticles go through a two-phase system (nanoparticle aggregation) and back to one-phase as a function of polymer (polyethylene glycol) concentration. Small-angle neutron scattering (SANS) studies have been carried out to examine the role of depletion interaction during this reentrant phase behavior responsible for the nanoparticle attraction, aggregation, and stabilization at low, intermediate, and high polymer concentrations, respectively [9]. SANS provides information on both the structure and interaction [27,28]. It is an ideal technique with the advantage of the easy possibility of contrast variation for such multicomponent systems [29–31]. The fact that neutron scattering is different for hydrogenated and deuterated solvents means that their mixed solvent has been selectively used to contrast-match polymer for directly studying the interaction between nanoparticles [32]. The interaction between the nanoparticles has been modeled using a two-Yukawa potential accounting for electrostatic repulsion between charged nanoparticles along with a polymer-induced depletion interaction [33–35]. The choice of Yukawa potentials is useful because it establishes the range and the strength of the individual parts (repulsive and depletion) of the total potential without any predefined assumption.

II. EXPERIMENT

Electrostatically stabilized colloidal suspensions of 30 wt% of silica nanoparticles (Ludox LS30) in water and polyethylene glycol (PEG) polymers having molecular weights 4, 6, and 20 K (kg/mol) were purchased from Sigma-Aldrich. Samples for pure nanoparticles and polymer systems were prepared by dissolving weighted amounts of silica and polymer in D_2O. For nanoparticle-polymer systems, samples were prepared in a mixed H_2O/D_2O (ratio 85/15) solvent for which polymer is contrast-matched to the solvent. Distilled de-ionized water from a Millipore MilliQ unit and 99.9% pure D_2O were used for sample preparation. All the measurements were carried out for fixed concentration (1 wt%) of silica nanoparticles with varying polymer concentration (0–5 wt%). Most of these measurements were carried out in the presence of $0.2M$ NaCl in order to reduce electrostatic repulsion between nanoparticles, so that it can be comparable with the depletion attraction where the particle clustering may be observed. Some measurements were also carried out to examine the role of varying salt concentration ($0-0.3M$ NaCl). Small-angle neutron scattering experiments were performed at the SANS-I facility, Swiss Spallation Neutron Source SINQ, Paul Scherrer Institut, Switzerland [36]. The wavelength (λ) of neutron beam used was 0.6 nm with a wavelength spread ($\Delta\lambda/\lambda$) of about 10%. The scattered neutrons from samples were detected using a two-dimensional 96 cm × 96 cm detector at two sample-to-detector distances of 2 and 8 m to cover data in a wave vector transfer [$Q = 4\pi \sin(\theta/2)/\lambda$, where θ is scattering angle] range of 0.04 to 3.0 nm^{-1}. Samples were held in Hellma quartz cells having a path length of 1 mm and the temperature was kept fixed at 30 °C during the measurements. Data were corrected for background and empty cell contributions and normalized to an absolute cross-sectional unit using standard procedure.

III. SMALL-ANGLE NEUTRON SCATTERING ANALYSIS

In SANS experiments, the coherent differential scattering cross section per unit volume ($d\Sigma/d\Omega$) is measured as a function of Q, and for a system of monodisperse particles can be expressed by [37–39]

$$\frac{d\Sigma}{d\Omega}(Q) = \phi V(\rho_p - \rho_s)^2 P(Q)S(Q) + B, \tag{1}$$

where ϕ is the volume fraction and V is particle volume. ρ_p and ρ_s are scattering length densities of particles and solvent, respectively. $P(Q)$ is the intraparticle structure factor and $S(Q)$ is the interparticle structure factor. B is a constant term denoting incoherent background from the sample.

$P(Q)$ is the square of the form factor and is decided by the geometry of the particle. For a sphere of radius R, $P(Q)$ is given by [40]

$$P(Q) = \left[\frac{3\{\sin(QR) - (QR)\cos(QR)\}}{(QR)^3}\right]^2. \tag{2}$$

$P(Q)$ for a polymer molecule as a Gaussian chain is given by [40]

$$P(Q) = 2\frac{\exp\left(-Q^2R_g^2\right) + Q^2R_g^2 - 1}{\left(Q^2R_g^2\right)^2}, \tag{3}$$

where R_g is the radius of gyration of a polymer molecule.

$S(Q)$ describes the interaction between the particles present in the system. It is the Fourier transform of the pair correlation function [$g(r)$] for the mass centers of the particles. The interaction between particles may be attractive or repulsive or a combination of both and can be calculated from the two-Yukawa potential accounting for both attraction and repulsion as given by [33,41]

$$\begin{aligned} U(r) &= \infty \quad \text{for} \quad 0 < r < \sigma \\ &= -K_1\frac{\exp\left\{-\alpha_1\left(\frac{r}{\sigma} - 1\right)\right\}}{\frac{r}{\sigma}} + K_2\frac{\exp\left\{-\alpha_2\left(\frac{r}{\sigma} - 1\right)\right\}}{\frac{r}{\sigma}} \\ &\quad \text{for} \quad r > \sigma, \end{aligned} \tag{4}$$

where K (in units of k_BT, k_B is the Boltzmann constant, and T is temperature) is proportional to the magnitude of the potential and $1/\alpha$ is proportional to the range of the potential. $S(Q)$ is obtained by solving the following Ornstein-Zernike (OZ) equation for $U(r)$ under the mean spherical approximation (MSA) closure relation [33]:

$$h(r) = c(r) + n\int c(\mathbf{r} - \mathbf{r}_1)h(r_1)d\mathbf{r}_1, \tag{5}$$

where n is the number density of particles, $c(r)$ is the direct correlation function, and $h(r)$ is the total correlation function. The functions $h(r)$ and $g(r)$ are related by $h(r) = g(r) - 1$.

For polydisperse systems, $d\Sigma/d\Omega$ in Eq. (1) may be modified as

$$\frac{d\Sigma}{d\Omega}(Q) = \int \frac{d\Sigma}{d\Omega}(Q,R)f(R)dR + B, \tag{6}$$

where $f(R)$ is the size distribution and is usually accounted by the following log-normal distribution:

$$f(R) = \frac{1}{R\sigma\sqrt{2\pi}} \exp\left[-\frac{\left(\ln\frac{R}{R_{\rm med}}\right)^2}{2\sigma^2}\right], \quad (7)$$

where $R_{\rm med}$ and σ are the median value and standard deviation, respectively. The mean and median values are related as $R_m = R_{\rm med}\exp(\sigma^2/2)$. For simplification, the integration in Eq. (6) is carried out over $P(Q)$, whereas $S(Q)$ is calculated for the mean size of the particle.

Usually, the particle aggregates are characterized by fractal structure. For a surface fractal, $S_{sf}(Q)$ is accounted by the following equation [42,43]:

$$S_{sf}(Q) = Q^{-1}\Gamma(5-D_s)\xi^{5-D_s}[1+(Q\xi)^2]^{\left(\frac{D_s-5}{2}\right)} \times \sin[(D_s-1)\tan^{-1}(Q\xi)], \quad (8)$$

where D_s is the surface fractal dimension and ξ is the maximum length up to which the fractal microstructure exists.

However, for $Q \gg 1/\xi$, $S_{sf}(Q)$ simplifies to [42,43]

$$S_{sf}(Q) \sim Q^{-(6-D_s)}. \quad (9)$$

The data analysis has been carried out by comparing the experimental scattering data with different theoretical models. Corrections for instrumental smearing were taken into account throughout the data analysis [40]. The modeled scattering profiles were smeared by the appropriate resolution function to compare with the measured data [44].

IV. RESULTS AND DISCUSSION

Figure 1 shows the SANS data of pure 1 wt% silica nanoparticles and PEG polymer ($M_W = 6$ kg/mol) in the presence of $0.2M$ NaCl in D_2O. Both the silica nanoparticles and polymers show typical features of the form factor $P(Q)$ governed scattering, where the form factor oscillation for silica

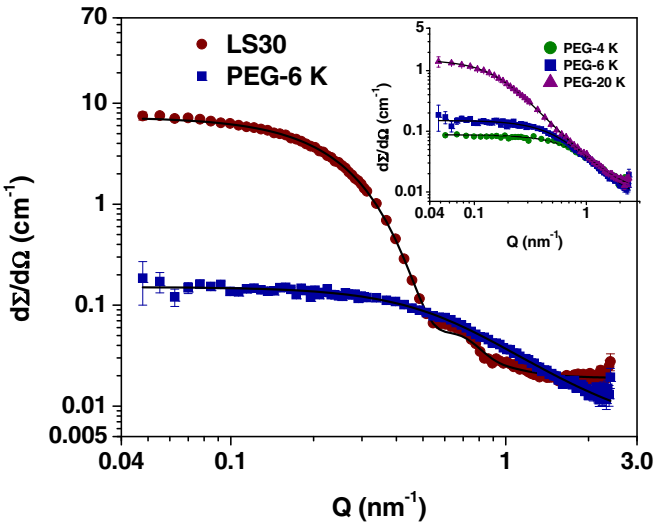

FIG. 1. (Color online) SANS data of 1 wt% LS30 silica nanoparticles and 1 wt% PEG-6 K ($M_W = 6$ kg/mol) polymer in presence of $0.2M$ NaCl in D_2O. Inset shows SANS data of 1 wt% polymers of different molecular weights.

TABLE I. Fitted structural parameters of 1 wt% silica nanoparticles and different molecular weight polymers

(a) Silica nanoparticle system		
Nanoparticle system	Mean radius R_m (nm)	Polydispersity σ
LS30	8.0	0.20
(b) Polymer systems		
Molecular weight (kg/mol)	Radius of gyration R_g (nm)	
4	2.2	
6	2.8	
20	5.5	

nanoparticles and $1/Q^2$ dependence for polymer at high Q data are observed [40]. This suggests that the interparticle structure $S(Q)$ contribution can be neglected in these systems. The nanoparticles have been modeled with polydisperse spheres having a mean size ($2R_m$) of 16.0 nm with a polydispersity (log-normal distribution) of 0.2 [34,45]. The radius of gyration (R_g) of PEG-6 K ($M_W = 6$ kg/mol) is found to be 2.8 nm using the Gaussian coil model [Eq. (3)]. The SANS data of other two different sized polymers having molecular weights 4 kg/mol (PEG-4 K) and 20 kg/mol (PEG-20 K) along with PEG-6 K are shown in the inset of Fig. 1. The cutoff of $1/Q^2$ dependence of polymer scattering in the low Q region (reciprocal of R_g) as expected shifts to lower Q values with the increase in the molecular weight. The calculated radii of gyration are 2.2 and 5.5 nm for PEG-4 K and PEG-20 K polymers, respectively (Table I). It may be mentioned that the variation of radius of gyration with molecular weight follows the relation $R_g\alpha(M_W)^\gamma$, where $\gamma = 0.61$ is found to be quite near the Flory exponent for real chains in good solvent [46]. The choice of sizes ($R_g < R_m/3$) of the polymers with respect to nanoparticles in the present study is varied within the range following the colloidal limit of the polymer-induced depletion interaction between nanoparticles [12,13].

An insight into the microscopic understanding of the effective polymer-induced interaction between nanoparticles can be obtained by studying the phase behavior of nanoparticles macroscopically as a function of polymer concentration. Figure 2 shows the phase behavior of 1 wt% LS30 silica nanoparticles with varying concentration of PEG-6 K in the presence of $0.2M$ salt (NaCl) in H_2O. The figure depicts the variation of the transmission of light through the silica nanoparticle system as a function of polymer concentration. It is observed that the value of transmission decreases dramatically from a clear solution (one-phase) after a critical concentration (~0.004 wt%) of polymer. The optical appearance of the system also shows turbidity (two phase) which increases with increasing polymer concentration. On further addition of polymer (>0.5 wt%), an increase in the transmitted light intensity is observed and the system regains its original behavior (one-phase). This variation of transmission of light may be related to the evolution of the structure in the system where the formation of larger structures will scatter more light and hence, the decrease in the transmission [47]. Based on this fact the phase behavior may be divided into three regimes of polymer concentration (Fig. 2).

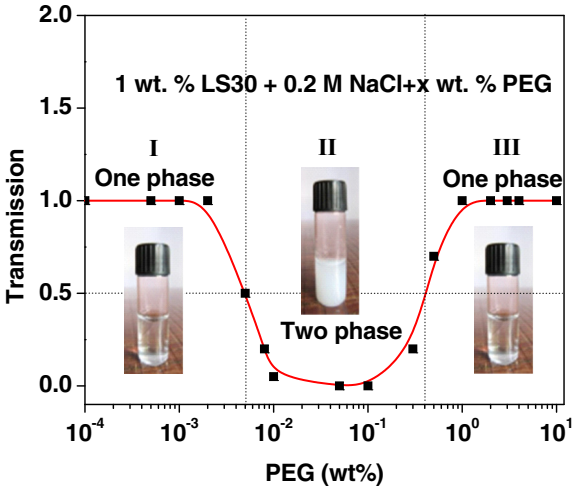

FIG. 2. (Color online) Phase behavior of 1 wt% LS30 silica nanoparticles with varying PEG concentration in the presence of 0.2M NaCl in H_2O. The figure depicts the transmission of light through the nanoparticle-polymer system with varying concentration of polymer. The insets show the physical state of the samples in different regimes of phase behavior.

The system converts from a charge stabilized one-phase nanoparticle system to a two-phase (nanoparticle aggregation) system in regime I, remains throughout in a two-phase system in regime II and returns back to a one-phase in regime III. Such reentrant phase behavior has stimulated interest in ascertaining the details of the responsible interactions.

The interplay of different interactions (electrostatic repulsion vs depletion attraction) and resultant structures in deciding the above phase behavior has been examined by SANS. Figure 3 shows the SANS data of 1 wt% silica nanoparticles in the presence of varying concentration of PEG-6 K in a H_2O/D_2O solvent (15% D_2O) for which PEG molecules are contrast matched. The SANS data are divided into three sets corresponding to three different polymer regimes of phase behavior in Fig. 2. The features of the scattering data are observed to be significantly different for the three data sets. In the first data set [Fig. 3(a)] where the nanoparticle-polymer system is converting from a one-phase to a two-phase system, there is a systematic buildup of scattering in the low Q region with data remaining almost similar in the intermediate and high Q values. The second data set [Fig. 3(b)] for a two-phase system shows a very large scattering intensity buildup in the low Q region followed by a Bragg peak at intermediate Q value. In the third set [Fig. 3(c)], the features of SANS data are quite similar to that of the first set. However, the buildup of scattering in the third set (unlike the first set) is suppressed with the increase in the polymer concentration as the two-phase system returns back to a one-phase system. Finally, the scattering profile at higher polymer concentration (5 wt%) is found to be overlapping with that of the pure nanoparticle system.

The buildup of scattering in the low Q region at low polymer concentrations [Fig. 3(a)] arises because of attractive interaction induced in the system [34,48]. The corresponding $S(Q)$ plots as calculated by dividing the data with those of nanoparticles without polymer are shown in Fig. 4 [34,49]. The

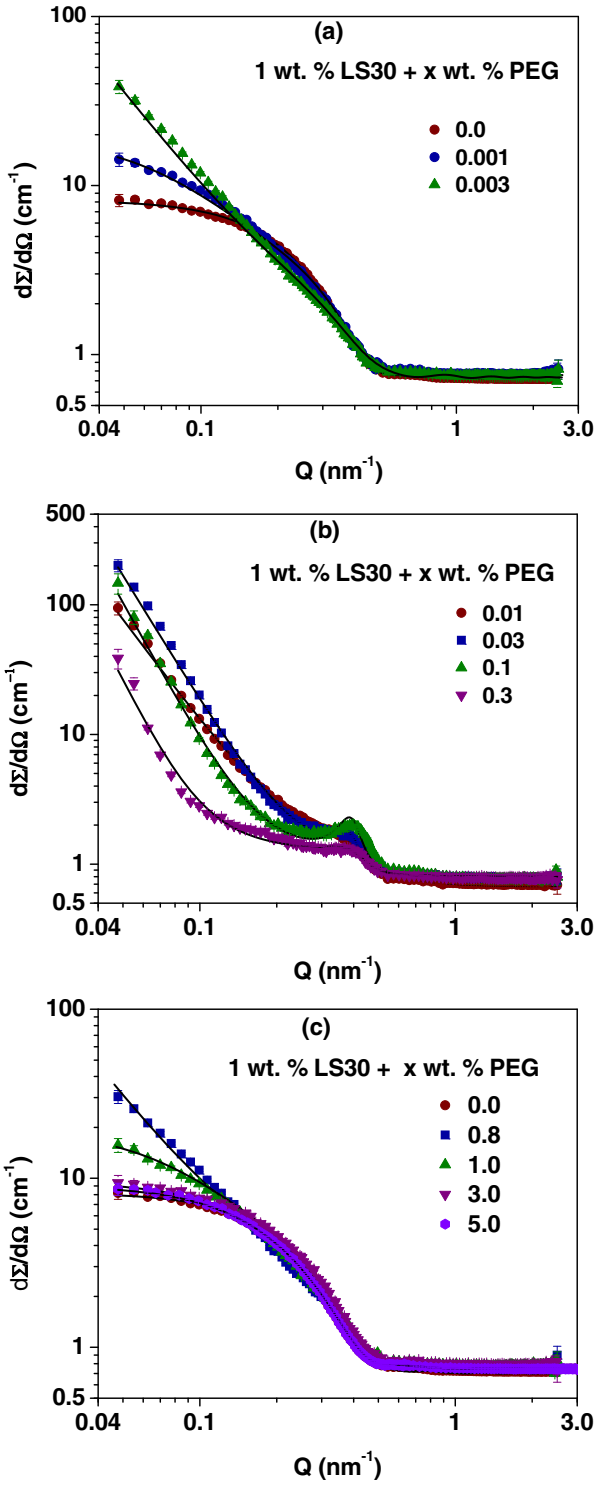

FIG. 3. (Color online) SANS data of 1 wt% silica nanoparticles with varying PEG-6 K polymer concentration (0–5.0 wt%) corresponding to three regions of phase behavior (Fig. 2).

diverging nature of $S(Q)$ in the low Q region and, in particular, the increase in the value of $S(Q = 0)$ clearly suggests enhancement in the attractive interaction with the increasing polymer concentration. The $S(Q)$ in this concentration regime has been calculated for a two-Yukawa potential [Eq. (4)] accounting for both attractive (depletion) and repulsive (electrostatic) forces

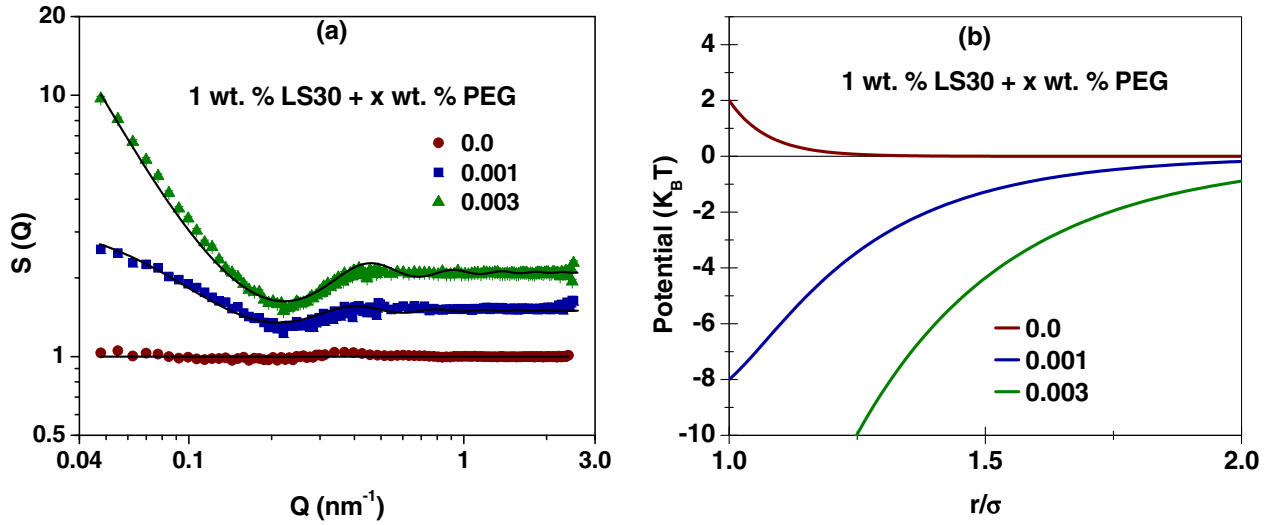

FIG. 4. (Color online) Variation of (a) structure factor and (b) total interaction potential for 1 wt% LS30 silica nanoparticles with varying PEG concentration (0–0.003 wt%). The data of the structure factor are shifted vertically for clarity.

in the system [32,33]. There are four unknown parameters, K_1, K_2, α_1, and α_2, in Eq. (4) [33,50]. The parameters K_1 and α_1 represent the magnitude and range ($1/\alpha_1$) of the attraction, respectively. On the other hand, the parameters K_2 and α_2 are related to effective charge (strength) and Debye length (ionic strength) of electrostatic repulsion [50]. The fact that no features of $S(Q)$ in nanoparticle solution without polymer were observed in the Q range of measurement means, therefore, that the parameters of repulsive interaction (K_2 and α_2) were determined from the extrapolation of concentrated nanoparticle solutions [47]. The values of K_2 and α_2 are found 2.0 k_BT and 12.5, respectively. These parameters were kept fixed during the analysis as the electrostatic part of the interaction on addition of polymer is expected to remain unchanged. Thus only parameters K_1 and α_1 corresponding to the depletion interaction were used as fitting parameters in $S(Q)$. The calculated resultant interaction potentials are plotted in Fig. 4(b). Both the magnitude of attraction (K_1) and the range ($1/\alpha_1$) (Table II) are found to be much larger than that of repulsion [34,51]. The strength of the attraction

TABLE II. Fitted parameters of interaction and structure for 1 wt% silica nanoparticles as a function of polymer (PEG) concentration.

(a) The evolution of depletion interaction in the regime of low polymer concentration. The parameters of repulsive interaction ($K_2 = 2$, $\alpha_2 = 12.5$) are fixed.

Polymer concentration (weight percent)	K_1 (k_BT)	α_1
0.0	–	–
0.001	10.0	3.0
0.003	24.0	2.6

(b) The structure of nanoparticle aggregates in the intermediate polymer concentration.

Polymer concentration (weight percent)	Surface fractal dimension D_s	Particle-particle distance d (nm)	Volume fraction φ
0.01	2.9	–	0.33
0.03	2.5	17.0	0.41
0.1	2.3	16.0	0.43
0.3	2.1	17.5	0.27

(c) The evolution of depletion interaction in the regime of high polymer concentration. The parameters of repulsive interaction ($K_2 = 2$, $\alpha_2 = 12.5$) are fixed.

Polymer concentration (weight percent)	K_1 (k_BT)	α_1
0.8	14.0	2.6
1.0	12.0	2.8
3.0	4.0	3.0
5.0	1.0	4.0

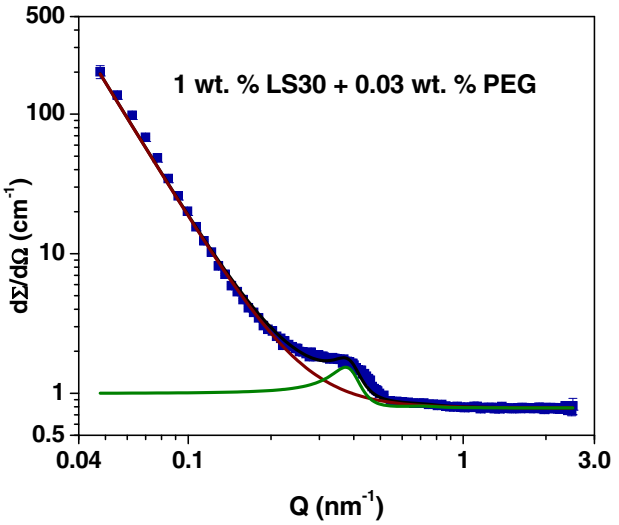

FIG. 5. (Color online) The fitted data of 1 wt% LS30 + 0.03 wt% PEG-6 K along with calculated contributions arising from nanoparticle aggregates (power law) and nanoparticles within aggregate (Bragg peak).

increases whereas the range remains almost the same with the increase in the polymer concentration. It is also found that the value of the interaction potential at an average distance has a value around 1.5 k_BT (average thermal kinetic energy) for 0.003 wt% of polymer, which is thereafter (higher polymer concentration) responsible for a one-phase system converting to a two-phase system in Fig. 2.

The SANS data [Fig. 3(b)] corresponding to a two-phase system (nanoparticle aggregation) show linearity in the low Q region indicating the fractal nature of nanoparticle clusters, whereas the Bragg peak around $Q_p = 0.4\,\mathrm{nm}^{-1}$ represents the ordered packing of nanoparticles within the aggregates [34,43,45]. The slopes of all the data in Fig. 3(b) in the low Q region have a value greater than 3, which implies that the scattering results from the surface fractal structure of the aggregates [43,45]. The average distance ($d \sim 2\pi/Q_p$) between the particles as calculated from the Bragg peak position is similar to the particle size suggesting the simple cubic-type packing of the particles within the clusters [34,52]. The second-order peak is not seen because of the high incoherent background and also low Q resolution in SANS at high Q values. The data have been fitted by the sum of power law behavior for a surface fractal [Eq. (9)] and the contribution from ordered particles within the clusters [Eq. (1)] [34,45]. The Bragg peak emerging as a result of interaction between the particles within the clusters is fitted through $S(Q)$ calculated from the analytical solution of the Ornstein-Zernike equation in the Percus-Yevick approximation (PYA), employing a hard sphere potential between the particles [34,53]. These two calculated contributions for typical data (polymer concentration of 0.03 wt%) are shown in Fig. 5. The fractal dimension ($Ds = 6 - m$, m is slope of the data) decreases with the increase in the polymer concentration [Fig. 3(b)], which may be explained based on the polymer concentration–dependent size of nanoparticle aggregates. The large size of the aggregates means smother surface, and hence lower surface fractal dimension. The volume fraction of the particles within the aggregates is found to be around 0.4, which could be because of deviations from perfect ordering (volume fraction = 0.53) [34]. There is suppression of scattering (polymer concentration 0.3 wt%) in the intermediate Q range which probably indicates the loosening of aggregates (signature of reentrant phase behavior) with increase in polymer concentration.

The SANS data approaching reentrant phase behavior [Fig. 3(c)] have also been analyzed using a two-Yukawa potential. The systematic decrease in the low Q data suggests that the attractive interaction between nanoparticles is now decreasing with the increasing polymer concentration. The structure factor and calculated potential of the data in Fig. 3(c) are shown in Fig. 6. The fitted parameters of the attractive potential are given Table II (c). It is clear that the strength of the attractive part decreases dramatically with increasing polymer concentration. The range of the attractive potential is also found to be decreasing at higher polymer concentrations. These results thus demonstrate that the change in depletion interaction dictates

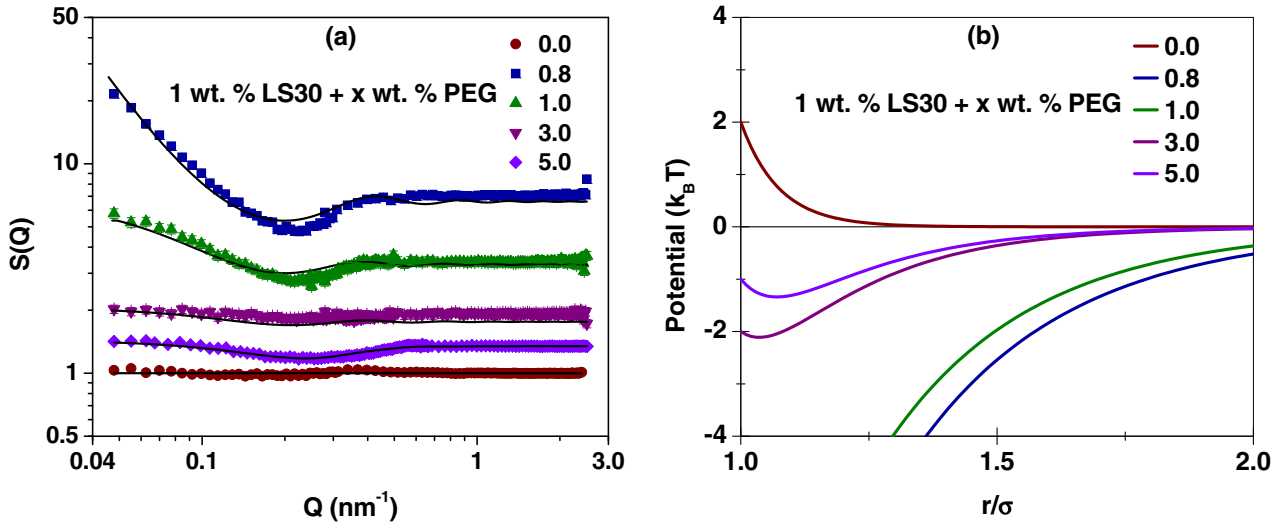

FIG. 6. (Color online) Variation of (a) structure factor and (b) total interaction potential for 1 wt% LS30 silica nanoparticles with varying PEG concentration (0.8–5.0 wt%). The data of the structure factor are shifted vertically for clarity.

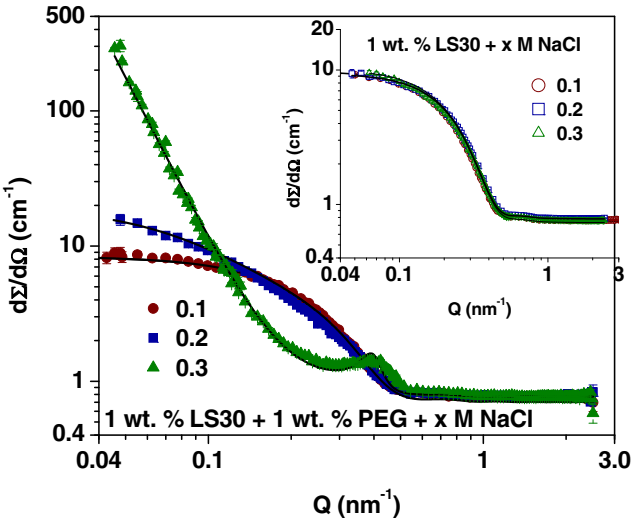

FIG. 7. (Color online) SANS data of 1 wt% silica nanoparticles with 1 wt% PEG-6 K polymer in the presence of varying salt (NaCl) concentration. Inset shows the SANS data of a nanoparticle system without any polymer in the presence of salt.

the reentrant phase behavior. Usually, the phase behavior in such systems is governed by the interplay of the following interactions present in the system (i) nanoparticle-nanoparticle electrostatic interaction, (ii) polymer-induced depletion interaction between nanoparticles, and (iii) polymer-polymer interaction. The electrostatic repulsion between nanoparticles is not expected to change much with increasing polymer concentration. However, at low polymer concentrations, the electrostatic repulsion dominates over the depletion attraction. The increase in polymer concentration enhances depletion attraction to give rise to the nanoparticle aggregation in a two-phase system. The reentrant of a one-phase system arises because of an increase in polymer-polymer repulsion at high polymer concentrations. This polymer-polymer interaction effectively tends to suppress the depletion attraction by forcing the system to do more work for expelling the polymer molecules from the depletion zones [11,54]. Moreover, at high polymer concentrations, the polymer chains between the particles are required to be transported against a very steep osmotic pressure gradient between the depletion region and the bulk, causing a stabilization effect [13,21]. It may be noted that the strength of the depletion attraction is not monotonically increasing with increasing polymer concentration. However, its nature remains attractive [Fig. 6]. There is a possibility of adsorption of polymer at high concentrations, resulting in steric stabilization of the nanoparticles. However, it is difficult to obtain this information from the present SANS measurements. The scattering when nanoparticles are contrast matched is dominated by individual polymers and high incoherent background, which makes it difficult to separate any significant contribution arising from the adsorbed polymers.

The degree of attractive and repulsive forces acting in the system decides the phase behavior [Fig. 2]. In the experiments discussed so far we have only tuned the attractive component of the interaction. The effect of varying the electrostatic repulsion and hence the total potential on the evolution of the structure and interaction of nanoparticles has been examined by varying the ionic strength of the solution. Figure 7 shows the SANS data of 1 wt% nanoparticles with 1 wt% PEG and varying salt concentration ($0.1M$ to $0.3M$ NaCl). The SANS data show significantly different features as the salt concentration is increased, suggesting that the interaction and structure in the system is being modified with the increasing salt concentration. The buildup of scattering in the low-Q region for salt concentration for $0.1M$ to $0.2M$ is because the total potential becomes more attractive on screening of the repulsion part. However, increase in the overall attractive potential for salt concentration $0.3M$ and beyond leads to nanoparticle aggregates (Table III). Charged colloids are known to undergo attractive interaction when ionic strength of the solution is increased [55], but no significant changes are observed in the data of nanoparticles with salt alone in the absence of any polymer (inset of Fig. 7), as the system may still be repulsive. The LS30 silica nanoparticle system shows salt-induced aggregation for NaCl concentration greater than $1M$. The structure of these salt-induced aggregates has the same morphology as found with the polymers. However, the system (salt-induced aggregation) does not show any reentrant phase behavior like with polymers.

The molecular weight of the polymer is known to be one of the strong parameters in tuning the polymer-induced depletion interaction. The excluded volume effect is enhanced with increasing polymer size and hence depletion interaction. SANS has been used to examine the effect of the molecular weight of the polymer on the phase behavior of the

TABLE III. Fitted parameters of the interaction and structure in nanoparticle-polymer (1 wt% LS30 + 1 wt% PEG-6 K) system with varying salt concentration.

(a) The calculated parameters of two-Yukawa potential prior to formation of two-phase system. formation of two-phase system.

Salt concentration (M)	K_1 (k_BT)	α_1	K_2 (k_BT)	α_2
0.1	12.0	3.0	3.0	9.0
0.2	12.0	2.8	2.0	12.5

(b) The structure of nanoparticle aggregates at high salt concentration.

Salt concentration (M)	Surface fractal dimension D_s	Particle-particle distance d (nm)	Volume fraction φ
0.30	2.2	16.8	0.45

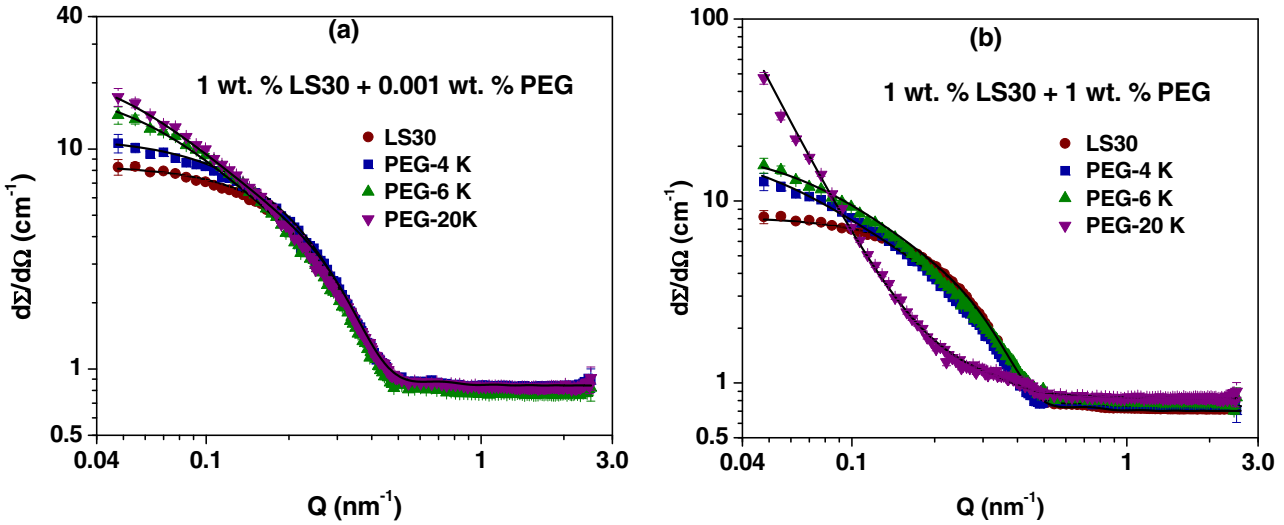

FIG. 8. (Color online) SANS data of 1 wt% silica nanoparticles with different molecular weight polymers (M_W = 4, 6, and 20 kg/mol) at (a) 0.001 and (b) 1.0 wt% concentrations of polymers.

nanoparticle-polymer system. Figure 8 shows SANS data of 1 wt% nanoparticles with three different molecular weight [4, 6, and 20 kg/mol] polymers in a one-phase system for polymer concentrations (a) prior to and (b) after the region of a two-phase system in phase behavior. The analysis (Table IV) shows that conversion from a one-phase to a two-phase system (increase in attractive depletion) is favored with the increase in the molecular weight of the polymer. However, the same is not the case in achieving the reentrant phase behavior. This is possibly because the polymer-polymer interaction is suppressed with increasing molecular weight (decrease in number density of polymer). Both the magnitude and range of depletion interaction are found to be increasing with the molecular weight of the polymer [12,13]. Thus, the present results show that the total interaction and resultant structure in a nanoparticle-polymer system can be tuned by varying polymer concentration, ionic strength, and molecular weight of the polymer.

V. CONCLUSION

The charged stabilized silica nanoparticles in the presence of PEG polymer show a reentrant phase behavior where nanoparticles go transition through a one-phase to a two-phase system and back to a one-phase system as a function of polymer concentration. The evolution of interaction and structure responsible for this phase behavior has been studied by SANS by contrast-matching the polymer. The phase behavior is found to be governed by the interplay of different interactions (i) electrostatic repulsion between nanoparticles, (ii) polymer-induced attractive depletion between nanoparticles and (iii) repulsive polymer-polymer interaction present in the system. At low polymer concentrations, the stability of this one-phase system is dictated by the dominance of electrostatic repulsion over the depletion attraction. On further addition of polymer, depletion attraction between nanoparticles sufficiently increases to give rise clustering of nanoparticles in two-phase system. The reentrant phase is

TABLE IV. Fitted parameters of 1 wt% silica nanoparticles with different molecular weight polymers (M_W = 4, 6, and 20 kg/mol) at (a) 0.001 and (b) 1.0 wt% concentrations of polymers.

(a) The comparison of depletion interaction for different polymers at 0.001 wt% concentration. The parameters of repulsive interaction ($K_2 = 2$, $\alpha_2 = 12.5$) are fixed.

Polymer molecular weight (kg/mol)	K_1 (k_BT)	α_1
4	8.0	3.5
6	10.0	3.0
20	12.5	2.3

(b) The comparison of depletion interaction for different polymers at 1.0 wt% concentration. The parameters of repulsive interaction ($K_2 = 2$, $\alpha_2 = 12.5$) are fixed. In the case of PEG-20 K, the reentrant phase is suppressed and the system is characterized by nanoparticle aggregates ($Ds = 2.2$).

Polymer molecular weight (kg/mol)	K_1 (k_BT)	α_1
4	9.0	3.4
6	10.0	3.0

driven by the reduction in depletion attraction as a result of polymer-polymer repulsion at higher polymer concentrations. The interaction between nanoparticles has been modeled by a two-Yukawa potential accounting for depletion as well as electrostatic interaction. Both the magnitude and range of depletion interaction increase in going from one-phase to two-phase system, whereas decrease back in the reentrant of one-phase system. The two-phase system is characterized by the nanoparticle clusters having surface fractal morphology. The role of varying electrostatic repulsion by ionic strength and depletion attraction by molecular weight of polymer has also been studied. The combination of these parameters (ionic strength and molecular weight of polymer) with polymer concentration decides the interaction and structure, which can be used to tune the reentrant phase behavior in nanoparticle-polymer systems.

[1] C. C. You, O. R. Miranda, B. Gider, P. S. Ghosh, I. B. Kim, B. Erdogan, S. A. Krovi, U. H. F. Bunz, and V. M. Rotello, Nat. Nanotechnol. **2**, 318 (2007).

[2] H. Zou, S. Wu, and J. Shen, Chem. Rev. **108**, 3893 (2008).

[3] G. Schmidt and M. M. Malwitz, Curr. Opin. Colloid Interface Sci. **8**, 103 (2003).

[4] Y. N. Pandey, G. J. Papakonstantopoulos, and M. Doxastakis, Macromolecules **46**, 5097 (2013).

[5] D. Aili, P. Gryko, B. Sepulveda, J. A. G. Dick, N. Kirby, R. Heenan, L. Baltzer, B. Liedberg, M. P. Ryan, and M. M. Stevens, Nano Lett. **11**, 5564 (2011).

[6] Q. H. Zeng, A. B. Yu, and G. Q. Lu, Prog. Polym. Sci. **33**, 191 (2008).

[7] O. Spalla, Curr. Opin. Colloid Interface Sci. **7**, 179 (2002).

[8] M. Zackrisson, A. Stradner, P. Schurtenberger, and J. Bergenholtz, Langmuir **21**, 10835 (2005).

[9] D. Ray and V. K. Aswal, J. Phys.: Condens. Matter **26**, 035102 (2014).

[10] R. Tuinier, J. Rieger, and C. G. De Kruifa, Adv. Colloid Interface Sci. **103**, 1 (2003).

[11] X. Ye, T. Narayanan, P. Tong, J. S. Huang, M. Y. Lin, B. L. Carvalho, and L. J. Fetters, Phys. Rev. E **54**, 6500 (1996).

[12] C. N. Likos, Phys. Rep. **348**, 267 (2001).

[13] H. N. W. Lekkerkerker and R. Tuinier, *Colloids and the Depletion Interaction* (Springer, Heidelberg, 2011).

[14] J. M. Mendez-Alcaraz and R. Klein, Phys. Rev. E **61**, 4095 (2000).

[15] S. Ramakrishnan, M. Fuchs, K. S. Schweizer, and C. F. Zukoski, J. Chem. Phys. **116**, 2201 (2002).

[16] S. Asakura and F. Oosawa, J. Chem. Phys. **22**, 1255 (1954).

[17] A. I. Chervanyov, Phys. Rev. E **83**, 061801 (2011).

[18] R. Tuinier, G. A. Vliegenthart, and H. N. W. Lekkerkerker, J. Chem. Phys. **113**, 10768 (2000).

[19] A. A. Shvets and A. N. Semenov, J. Chem. Phys. **139**, 054905 (2013).

[20] D. Rudhardt, C. Bechinger, and P. Leiderer, J. Phys.: Condens. Matter **11**, 10073 (1999).

[21] R. I. Feigin and D. H. Napper, J. Colloid Interface Sci. **75**, 525 (1980).

[22] J. Y. Walz and A. Sharma, J. Colloid Interface Sci. **168**, 485 (1994).

[23] G. K. James and J. Y. Walz, J. Colloid Interface Sci. **418**, 283 (2014).

[24] P. B. Warren, S. M. Ilett, and W. C. K. Poon, Phys. Rev. E **52**, 5205 (1995).

[25] M. Schmidt, A. R. Denton, and J. M. Brader, J. Chem. Phys. **118**, 1541 (2003).

[26] G. J. Fleer and J. M. H. M. Scheutjens, Croat. Chem. Acta **60**, 477 (1987).

[27] C. Wu, T. J. Cho, J. Xu, D. Lee, B. Yang, and M. R. Zachariah, Phys. Rev. E **81**, 011406 (2010).

[28] S. Kumar and V. K. Aswal, J. Phys.: Condens. Matter **23**, 035101 (2011).

[29] D. I. Svergun and M. H. J. Koch, Rep. Prog. Phys. **66**, 1735 (2003).

[30] M. Granite, A. Radulescu, W. Pyckhout-Hintzen, and Y. Cohen, Langmuir **27**, 751 (2011).

[31] T. Zemb and E. Leontidis, Curr. Opin. Colloid Interface Sci. **18**, 493 (2013).

[32] S. Kumar, V. K. Aswal, and J. Kohlbrecher, Langmuir **28**, 9288 (2012).

[33] Y. Liu, W.-R. Chen, and S.-H. Chen, J. Chem. Phys. **122**, 044507 (2005).

[34] S. Kumar, M.-J. Lee, V. K. Aswal, and S.-M. Choi, Phys. Rev. E **87**, 042315 (2013).

[35] A. Shukla, E. Mylonas, E. Cola, S. Finet, P. Timmins, T. Narayanan, and D. Svergun, Proc. Natl. Acad. Sci. USA **105**, 5075 (2008).

[36] J. Kohlbrecher and W. Wagner, J. Appl. Crystallogr. **33**, 804 (2000).

[37] S. H. Chen, E. Y. Sheu, J. Kalus, and H. Hoffmann, J. Appl. Crystallogr. **21**, 751 (1988).

[38] J. B. Hayter and J. Penfold, Colloid Polymer Sci. **261**, 1022 (1983).

[39] C. G. Windsor, J. Appl. Cryst. **21**, 582 (1988).

[40] J. S. Pedersen, Adv. Colloid Interface Sci. **70**, 171 (1997).

[41] Y. Liu, E. Fratini, P. Baglioni, W.-R. Chen, and S.-H. Chen, Phys. Rev. Lett. **95**, 118102 (2005).

[42] A. P. Radlinski, E. Z. Radlinska, M. Agamalian, G. D. Wignall, P. Lindner, and O. G. Randl, Phys. Rev. Lett. **82**, 3078 (1999).

[43] D. F. R. Mildner and P. L. Hall, J. Phys. D: Appl. Phys. **19**, 1535 (1986).

[44] P. R. Bevington, *Data Reduction and Error Analysis for Physical Sciences* (McGraw-Hill, New York, 1969).

[45] S. Kumar, V. K. Aswal, and P. Callow, Langmuir **30**, 1588 (2014).

[46] I. Teraoka, *Polymer Solutions: An Introduction to Physical Properties* (John Wiley & Sons, Inc., New York, 2002).

[47] I. Yadav, S. Kumar, V. K. Aswal, and J. Kohlbrecher, Phys. Rev. E **89**, 032304 (2014).

[48] T. Sato, T. Komatsu, A. Nakagawa, and E. Tsuchida, Phys. Rev. Lett. **98**, 208101 (2007).

[49] X. Ye, T. Narayanan, P. Tong, and J. S. Huang, Phys. Rev. Lett. **76**, 4640 (1996).
[50] A. J. Chinchalikar, V. K. Aswal, J. Kohlbrecher, and A. G. Wagh, Phys. Rev. E **87**, 062708 (2013).
[51] W. Knoben, N. A. M. Besseling, and M. A. Cohen Stuart, Phys. Rev. Lett. **97**, 068301 (2006).
[52] T. G. Shin, D. Müter, J. Meissner, O. Paris, and G. H. Findenegg, Langmuir **27**, 5252 (2011).
[53] N. W. Ashcroft and J. Lekner, Phys. Rev. **145**, 83 (1966).
[54] W. C. K. Poon, J. Phys.: Condens. Matter **14**, R859 (2002).
[55] A. J. Chinchalikar, V. K. Aswal, J. Kohlbrecher, and A. G. Wagh, Chem. Phys. Lett. **542**, 74 (2012).